



Full Length Article

The Effect of the Method of Adding Impregnation Solutions on the Properties and Performance of the Pd-Ag/Al₂O₃ Catalyst in the Tail-End Acetylene Selective Hydrogenation

M. Takht Ravanchi*, S. Sahebdehfar, M. Rahimi Fard, H. Moosavi

Catalyst Research Group, Petrochemical Research and Technology Company, National Petrochemical Company, Tehran, Iran

ARTICLE INFO

Article history:

Received: 2021-06-07

Accepted: 2021-08-05

Available online: 2022-02-06

Keywords:

Palladium Catalyst,
Impregnation,
Recycle Reactor,
Acetylene Selective
Hydrogenation

ABSTRACT

The impregnation of the alumina support with the PdCl₂ solution was investigated in batch and semi-batch operation modes using a recycle packed-bed reactor. The UV-visible analysis was used to evaluate the kinetics of the adsorption of Pd on the alumina support. The adsorption data related to transient palladium showed that the adsorption of Pd was very rapid and completed within few minutes. Bi-metallic Pd-Ag/Al₂O₃ catalysts were synthesized by the sequential impregnation method. CO-chemisorption, CO-TPD and FE-SEM tests were used to characterize the synthesized bi-metallic samples. The catalytic performance of the samples was evaluated for the tail-end acetylene selective hydrogenation process in a fixed-bed reactor. Moreover, the deactivation of the catalysts was evaluated mathematically by the integral method of analysis, considering reaction kinetics as power laws in terms of n^{th} orders in H₂ and C₂H₂ partial pressures. It was observed that by the batch-wise addition of the Pd precursor solution, a sample, with the lowest amount of Pd dimmers that had the highest ethylene selectivity and lowest hydrogenation reaction rate, was obtained.

DOI: 10.22034/ijche.2021.269052.1382 URL: http://www.ijche.com/article_144319.html

1. Introduction

In petrochemical industries, the selective hydrogenation of acetylene to ethylene is used for the removal of acetylene impurities from C₂= streams. The content acetylene must be reduced to 1-5 ppm; as it is the poison of the Ziegler-Natta catalyst in the downstream

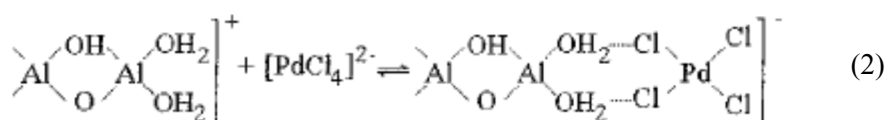
polymerization unit. In commercial plants, the acetylene selective hydrogenation process is performed as either the “front-end” or the “tail-end” configuration [1].

Generally, palladium is used as the active phase of the catalyst. As palladium has a limited selectivity and poor long-term

*Corresponding author: m.ravanchi@npc-rt.ir (M. Takht Ravanchi)

stability, bimetallic Pd catalysts have been used since 1980's. During the years, different researchers have used various metals (such as Ag, Na, Ga, Au, Sn, Bi, Sb, B, Ni, Cu, Pb, Cr, and K) as promoters of this catalyst [2, 3]. In recent years, Ag has been used as the promoter in commercial catalysts. Generally, Ag has three promotional effects; isolating the Pd active site and decreasing the coordination number of Pd atoms (geometric effect), reducing the hydride formation (kinetic effect) and being alloyed with Pd thereby modifying its electronic structure (electronic effect) [4-7].

In the preparation of the supported catalyst, the adsorption of PdCl_4^{2-} on alumina is an



This structure of PdCl_4^{2-} is preserved after adsorption.

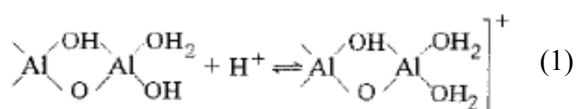
As the adsorption of Pd on the alumina support is the determining step in the synthesis of the catalyst, in the present research, the effect of different modes of the addition of Pd has been studied in detail and the effects of them on the morphology of the catalyst and its performance and deactivation were evaluated for the tail-end acetylene selective hydrogenation process. To the best of our knowledge, there is not any published research in which the kinetic adsorption of Pd has been evaluated on alumina supports.

2. Experimental

2.1. Chemicals

The spherical γ -alumina (2 mm in diameter), with a 210 m^2/g surface area and 0.5 cm^3/g pore volume, supplied by Sasol Company after having been pre-treated at 1090 $^\circ\text{C}$ for 3 h and with the heating rate of 5 $^\circ\text{C}/\text{min}$, was

important step, as it determines the distribution of the active metal in the final catalyst. In the acidic pH range, PdCl_4^{2-} is adsorbed onto the protonated surface of the alumina support (via an electrostatic mechanism) [8]. Firstly, a fast protonation of alumina surface occurs (Eq. 1):



Then PdCl_4^{2-} is adsorbed on positively charged alumina surface sites (Al-OH_2^+) (Eq. 2):

used as the catalyst support.

Palladium chloride (PdCl_2) and silver nitrate (AgNO_3) were used as Pd and Ag precursors respectively. Those precursors were of commercial grade, supplied by Padideh Sazan Shimi Company and used without further treatment.

Acetylene-ethylene gas mix (with 1.5 mol. % of acetylene and 98.5 mol. % of ethylene), hydrogen (99.9 mol. %) and nitrogen (99.9 mol. %) cylinders were supplied by Dayan Gas Company and used as the reactant or diluent gases.

2.2. Catalyst synthesis

For studying the kinetics of the adsorption of palladium on alumina support, a double-wall tubular fixed bed quartz reactor accompanying two peristaltic pumps (with a 40 cm^3/min flow rate) for the circulation of the impregnation solution has been used. To ensure a proper distribution of the fluid flow,

the space below the alumina support bed was packed with 2 mm inert glass balls. A schematic diagram of the experimental set-up is provided elsewhere [9]. For this reactor, the height/diameter ratio of the support bed was 5.

For this experimental set-up, as the radial aspect ratio (i.e. the bed diameter to the catalyst particle diameter) is > 15 , channeling effects are negligible. On the other hand, dispersion effects are also negligible as the axial aspect ratio (i.e. the ratio of the catalyst bed length to the catalyst particle diameter) is > 30 [10].

The final target catalyst of the present research was the bimetallic Pd-Ag/Al₂O₃ catalyst. As the first step, Pd was impregnated on an alumina support (described above in the set-up) at 40 °C. In the second step, Ag was impregnated on Pd/Al₂O₃ samples in a rotary equipment at 25 °C. After each impregnation step, the samples were dried in an oven (Heraeus UT 6P) at 110 °C overnight and calcined in a furnace (Carbolite-CWF 13/13) in air at 450 °C for Pd and 400 °C for Ag.

In the present research, three different modes

$$0.024-0.3 \text{ mmol}_{\text{Pd}}/\text{L}_{\text{solution}}: y=0.3798x+0.00019 \quad (3)$$

$$0.3-2.4 \text{ mmol}_{\text{Pd}}/\text{L}_{\text{solution}}: y=0.28359x+0.03829 \quad (4)$$

where x is the concentration of Pd and y is its absorbance.

For studying the adsorption kinetic, the concentration of Pd in the impregnation solution was determined by recycling the solution into the quartz cell and measuring the absorbance at 432 nm against the reagent blank (appropriate amount of HCl in H₂O).

In order to determine the Pd dispersion in catalyst samples, a CO chemisorption analysis was performed. At first, the catalyst was

for the addition of the Pd precursor solution were considered, as below:

- Sample A: a batch-wise impregnation in which the Pd solution was added in one step to the circulating solution in a beaker containing DM (demineralized) water.
- Sample B: a semi-batch impregnation in which the Pd solution was added in four steps every 15 min to DM water inside the beaker including the circulating solution.
- Sample C: a semi-batch impregnation in which the Pd solution was added in 32 steps every 1 min to DM water inside the beaker including the circulating solution.

It is worth mentioning that for each sample, 40 g of the support was loaded in the impregnation reactor.

2.3. Catalyst characterization

In order to determine the concentration of palladium in the impregnation solution, a UV-Visible (T90, PG Instruments Limited Co.) apparatus was used. Through using different concentrations of Pd, calibration curves were constructed in two different ranges as below:

pre-treated in a reactor with 50 mL/min of hydrogen at 400 °C for 15 min. Afterwards, the reactor was connected to a BELCAT apparatus (type A) and cooled down to 50 °C by passing 50 mL/min of helium. Then, pulses of 1.009 mL of CO were introduced to the reactor every 1 min. A thermal conductivity detector (TCD) recorded the CO-signals. It is worth mentioning that CO is selectively chemisorbed on the Pd surface.

The analysis of the metal penetration depth

was performed with a field emission scanning electron microscope (FE-SEM) using an MIRA3 TESCAN apparatus. Each spherical pellet was polished on the top surface whereby half of the active Pd egg-shell was revealed. Then, the pellet was covered with an Au layer and transferred into the microscope. The measurements were carried out under high vacuum and with an electron beam having a voltage of 15 kV. The depth of the Pd-layer was read out from FE-SEM images.

For the CO temperature-programmed desorption (CO-TPD), the catalyst sample was loaded to the reactor of the BELCAT A apparatus, reduced by hydrogen at 150 °C for 2 h, and purged with helium at 150 °C for 1 h to remove the adsorbed H₂ from the Pd surface. Afterwards, the catalyst was exposed to CO at 40 °C and temperature was raised from 40 °C to 700 °C at a rate of 10 °C/min in helium.

The thermogravimetric and differential thermal analysis (TG-DTA) measurements of the used catalysts were performed using a Perkin Elmer SII apparatus (model: Diamond TG/DTA) in the temperature range of 25-800 °C. The temperature scanning rate was 5 °C/min.

2.4. Reaction study

The synthesized samples were evaluated for the acetylene selective hydrogenation (tail-end) in a high-pressure set-up, of which the detailed explanation is provided elsewhere [11].

In each test, 4 g of the catalyst diluted with the same size of quartz was loaded. The catalyst was first reduced with hydrogen in situ and at a GHSV of 500 h⁻¹ and temperature of 150 °C. Afterwards, the reactor was cooled down to the reaction temperature (60 °C) by nitrogen. Each catalyst was evaluated in the

presence of 1 mol. % C₂H₂, 1.5 mol. % H₂, 30 mol. % N₂ and C₂H₄ as balance (as feed) at 10 bar and the GHSV of 4000 h⁻¹. For analyzing the components of feed and product streams, an on-line gas chromatograph (Varian-CP-3800), equipped with FID and TCD detectors, was used.

The acetylene conversion (Eq. (5)) and ethylene selectivity (Eq. (6)) are parameters used for the evaluation of the performance of the catalyst.

$$X_{C_2H_2} = \frac{C_{C_2H_2,0} - C_{C_2H_2}}{C_{C_2H_2,0}} \quad (5)$$

$$S_{C_2H_4} = \frac{C_{C_2H_4} - C_{C_2H_4,0}}{C_{C_2H_2,0} - C_{C_2H_2}} \quad (6)$$

where C_i denotes the concentration of species i, 0 refers to the inlet condition, X is conversion and S is selectivity.

3. Mathematical modeling

Catalyst performance data can be evaluated quantitatively by using suitable kinetic models for the main reaction and catalyst deactivation. For an acetylene selective hydrogenation, normally, reaction kinetics is reported as power laws in terms of nth orders in H₂ and C₂H₂ partial pressures. It was reported that for hydrogen 0.5th, 1st and 1.5th orders could be used and for acetylene at low concentrations (that is the case for the tail-end configuration), a 1st order dependence was reported [12].

In the present research, the following rate expression has been used for the main reaction:

$$-r_A = akC_A C_B^{0.5} \quad (7)$$

where $-r_A$ is the disappearance rate for species A is per catalyst mass (mol/(kg.h)), a is the catalyst activity, k is the reaction rate constant

($\text{m}^{7.5}/\text{kg}\cdot\text{mol}^{0.5}\cdot\text{h}$), C_A is the concentration of acetylene (mol/m^3) and C_B is the concentration of hydrogen (mol/m^3).

In the tail-end acetylene selective hydrogenation, the concentration of acetylene

$$\frac{dX_A}{d(W/F_{A0})} = akC_{A0}^{1.5}(1 - X_A)(\mathcal{H} - X_A)^{0.5} \quad (8)$$

where X_A is the acetylene conversion, W is the catalyst weight (kg), F_{A0} is the molar flow rate (mol/h) of acetylene, C_{A0} the concentration (mol/m^3) of the inlet acetylene

$$k\tau C_{A0}^{0.5} = \int \frac{dX_A}{a(1-X_A)(\mathcal{H}-X_A)^{0.5}} \quad (9)$$

where τ is the catalyst weight per volumetric feed flow rate, v (m^3/h).

For the deactivation rate, a 2nd order kinetics is considered. The below correlation is obtained for the catalyst activity as a function of time:

$$a = \frac{1}{1+k_d t} \quad (10)$$

where k_d is the deactivation rate constant (h^{-1}).

Combining Eqs. (9) and (10), the conversion-time dependence is obtained as below:

$$\frac{k\tau C_{A0}^{0.5}}{1+k_d t} = \int \frac{dX_A}{(1-X_A)(\mathcal{H}-X_A)^{0.5}} \quad (11)$$

Upon integration along the reactor length and algebraic manipulations, Eq. (12) is obtained:

$$\frac{\tau C_{A0}^{0.5}(\mathcal{H}-1)^{0.5}}{\ln\left(\frac{(1+\alpha)(1-\alpha_0)}{(1-\alpha)(1+\alpha_0)}\right)} = \frac{k_d}{k} t + \frac{1}{k} \quad (12)$$

where $\alpha = \left(\frac{\mathcal{H}-X_A}{\mathcal{H}-1}\right)^{0.5}$ and $\alpha_0 = \left(\frac{\mathcal{H}}{\mathcal{H}-1}\right)^{0.5}$.

By plotting the left-hand-side (LHS) of Eq. (12) vs. t , a straight line was obtained from which k and k_d could be determined from the intercept and slope of the resulting line

in the feed is low; hence, the volume change of the reaction can be ignored. For a differential element of the catalyst weight in the reactor:

and \mathcal{H} is the hydrogen to acetylene molar ratio in the feed (mol/mol).

As $F_{A0} = vC_{A0}$, Eq. (8) yields:

respectively.

4. Results and discussion

4.1. Catalyst characterization

The concentrations of the impregnation solutions as the measure of the adsorption kinetics of Pd on the alumina support (in the first stage of the synthesis of Pd-Ag/ Al_2O_3 catalyst) are depicted for all synthesized samples in Figure 1. As it is obvious, the palladium adsorption on the alumina support, used in the present research, is very rapid and high. As it is observed in Figure 1a for sample A, within less than 20 min, Pd was totally adsorbed and after that time no Pd was detected in the circulating solution. When the Pd solution was added in a stepwise manner (samples B and C), high concentrations of Pd persisted in the impregnation solution for longer times (Figures 1b and 1c) and the support was contacted with the Pd precursor gradually.

The dispersion, surface area, and the concentration of the active site of palladium for synthesized Pd-Ag/ Al_2O_3 samples are tabulated in Table 1. As it is observed, when Pd has been added in four portions (i.e.

sample B), the highest Pd dispersion has been obtained which is equivalent to the smallest

Pd particle size. Moreover, this sample has the highest Pd surface area and active sites.

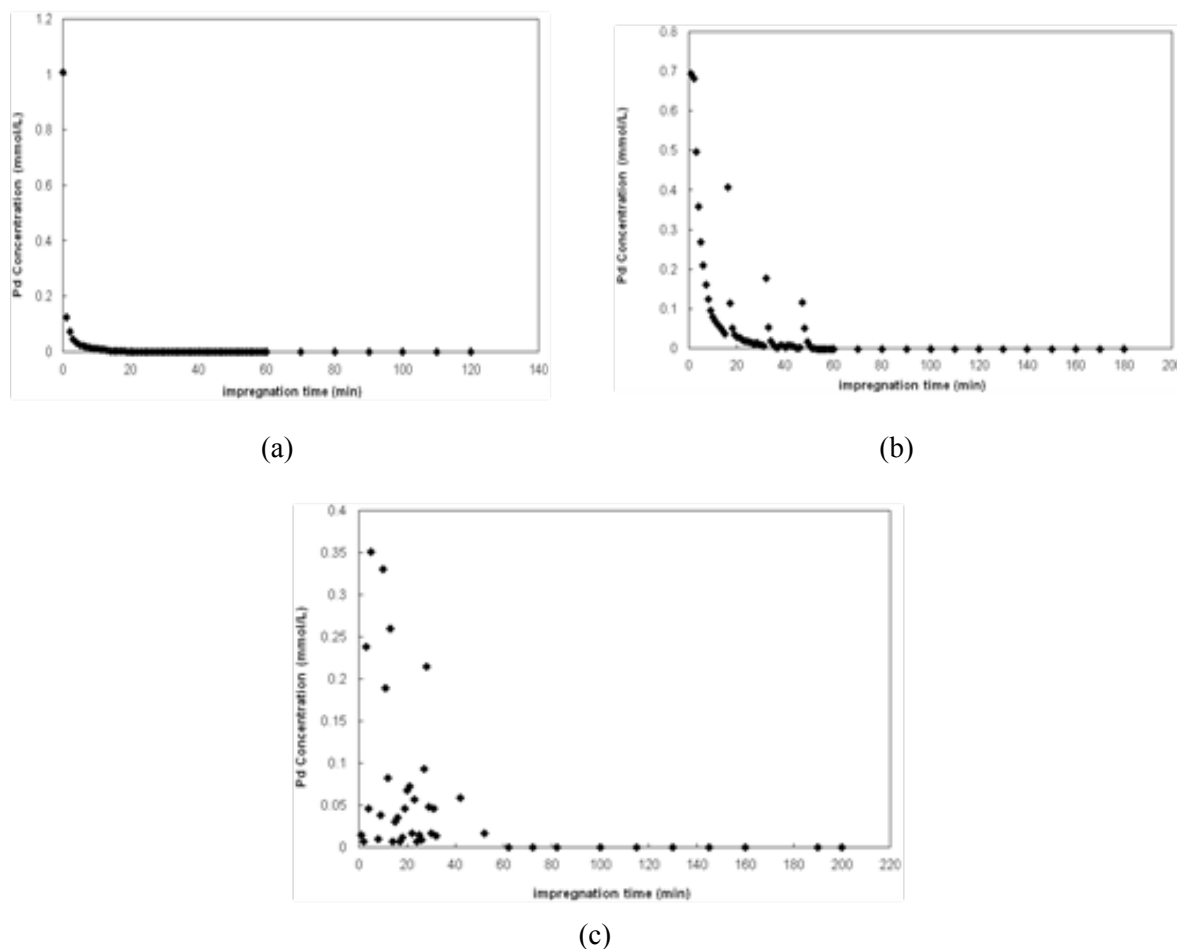


Figure 1. Transient adsorption of Pd on the alumina support; (a) Sample A, (b) Sample B and (c) Sample C.

Table 1

Pd dispersion, Pd active sites and Pd penetration depth for Pd-Ag/Al₂O₃ catalysts.

Sample	Pd dispersion (%)	Pd surface area (m ² /g)	Pd active sites (×10 ¹⁷ site/g _{catalyst})	Pd penetration depth (μm)
A	54.45	243.43	8.61	9.75
B	62.13	277.73	9.84	10.81
C	52.26	233.64	8.26	12.99

Palladium penetration depths for Pd-Ag/Al₂O₃ synthesized samples are also tabulated in Table 1. While the egg-shell distribution of Pd is prevailing, a slight and gradual increase in the penetration depth from sample A to C (in which the addition rate of

the PdCl₄²⁻ precursor to the impregnation solution was decreased) is observed. This implies that the strong intra-particle diffusion effect during impregnation could not be overcome by changing the concentration of the impregnation solution around the catalyst

pellet. In other words, both rates of the adsorption and diffusion of the Pd precursor in support pores increase in the same order as in the concentration of the adsorbing species; which is a characteristic of first-order adsorption kinetics.

TPD-CO results for Pd-Ag/Al₂O₃ synthesized samples are presented in Table 2 and Figure 2. All samples showed three desorption peaks corresponding to different palladium adsorption sites. When the Pd solution was added to DM water in a stepwise manner (samples B and C), in comparison to the same in the single-step manner (sample A), the first peak shifted to higher temperatures which showed a stronger adsorption of CO on the related Pd atoms. It is predicted that the adsorption strength of unsaturated hydrocarbons on these Pd sites

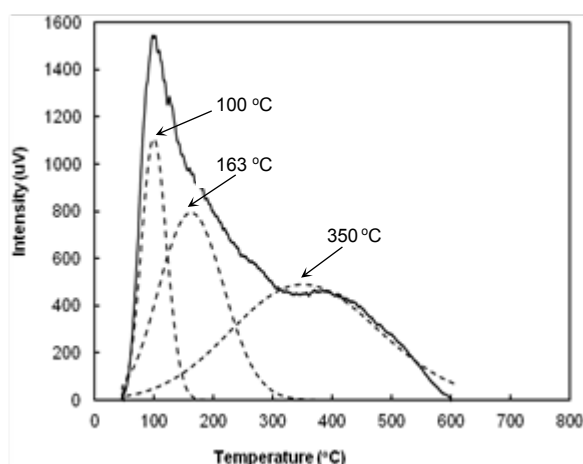
would also be higher in samples B and C, and consequently, the ethylene selectivity would decrease. Among the stepwise modes of the addition of Pd, when Pd was added in a high volume (sample B), the shift in the temperature of the first peak was higher; consequently, the resulting sample should have Pd sites with the strongest ethylene adsorption.

According to Table 2, sample A has the lowest CO consumption on 2nd and 3rd peaks, which is equivalent to the lowest amount of Pd dimmers on this sample. As these peaks are attributed to Pd dimmers which are responsible to bridge adsorption sites [13, 14], their lower amount is equivalent to a higher ethylene selectivity for this sample. Hence, it is predicted that sample A would exhibit the highest ethylene selectivity.

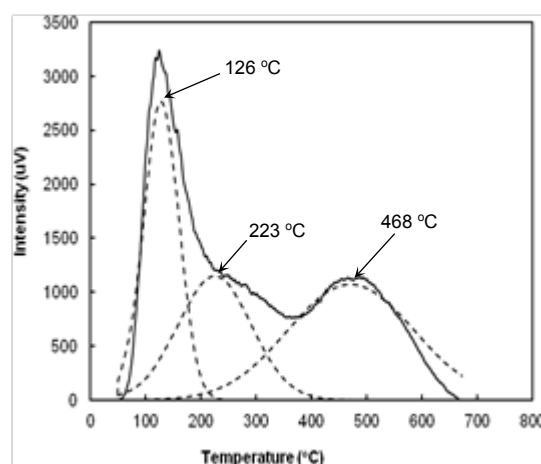
Table 2

CO consumption of Pd-Ag/Al₂O₃ catalysts.

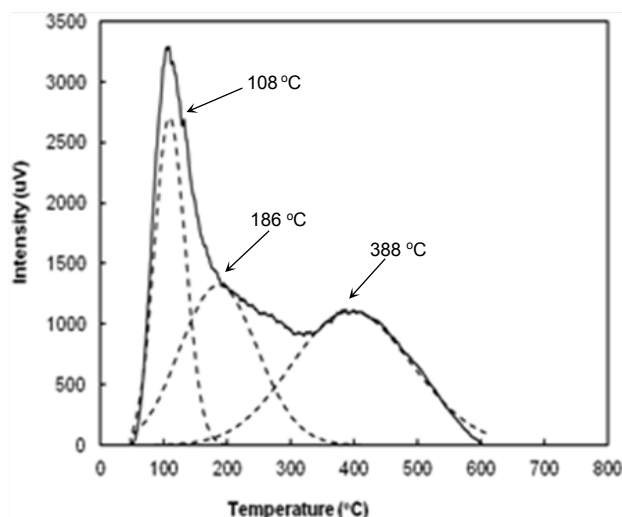
Sample	CO consumption (mmol/g)		
	First peak	Second peak	Third peak
A	0.034	0.058	0.076
B	0.111	0.098	0.150
C	0.094	0.110	0.131



(a)



(b)



(c)

Figure 2. TPD-CO graphs of Pd-Ag/Al₂O₃ catalysts; (a) Sample A, (b) Sample B and (c) Sample C.

4.2. Catalyst performance

Catalytic performance of the synthesized samples is presented in Figure 3. Among these samples, sample C had the lowest initial C₂H₄ selectivity. That sample had the lowest dispersion and highest Pd penetration depth as well (Table 1). A low dispersion is equivalent to a larger Pd particle size which is not suitable for an acetylene selective hydrogenation reaction; as it shifts the reaction to the ethylene hydrogenation pathway by which the ethylene selectivity is reduced.

It has been observed (Figure 3) that when the Pd precursor solution was added in a stepwise manner and in its lowest amount (sample C), the highest acetylene conversion was obtained. From another viewpoint, the highest acetylene conversion was obtained by the sample that had the lowest Pd dispersion and highest Pd penetration depth.

4.3. Catalyst deactivation

For all synthesized samples, plots of Eq. (12) are depicted in Figure 4. Fair fits were

observed for all samples. The kinetic parameters (k and k_d) of each catalyst are tabulated in Table 3. As it is observed, the catalyst activity decreases in the order of $C > B > A$ and stabilities are in the order of $C \approx A > B$.

It is worth mentioning that Hüttig and Tamman temperatures for Pd are 280 °C and 650 °C respectively. As the reduction and reaction temperatures were 150 °C and 60 °C, respectively, sintering could not be a mechanism of the catalyst deactivation.

According to the literature, the formation of heavy carbonaceous compounds, “coke”, is the main cause of the catalysts deactivation [12, 15]. Furthermore, it was reported that coke modified edge and corner sites (that are low coordinated Pd surface sites) after which the hydrogenation rate was increased [13]. Referring to Table 3, sample C has highest k_d . It is predicted that this sample has the highest hydrogenation rate which is validated by the higher rate constant of reaction for this sample (Table 3).

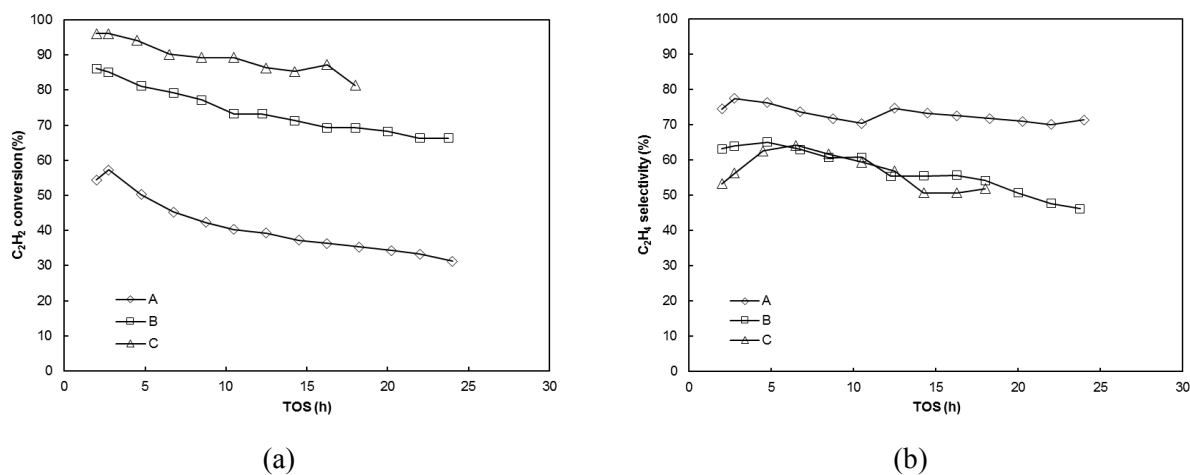


Figure 3. Catalytic performance of the synthesized samples.

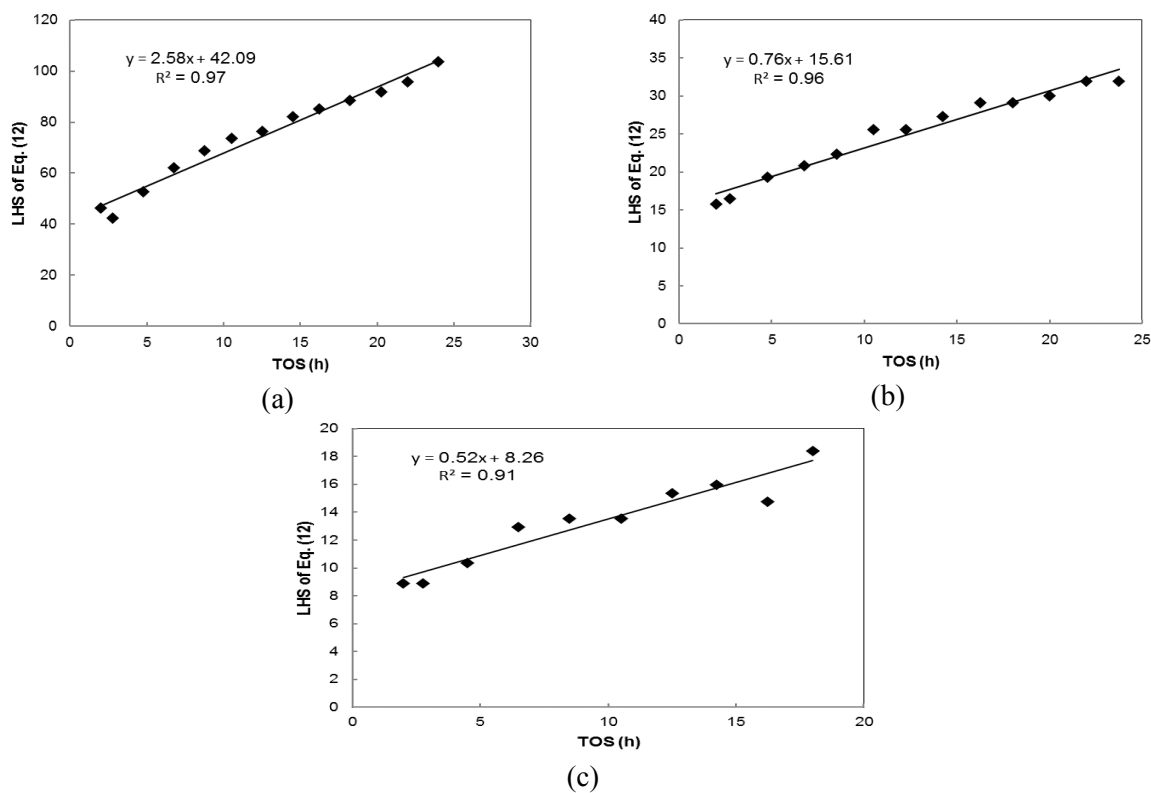


Figure 4. Plots of Eq. (12) for synthesized samples; (a) Sample A, (b) Sample B and (c) Sample C.

Table 3

Reaction and deactivation rate constant.

Sample	k ($m^{7.5}/kg.h.mol^{0.5}$)	k_d (h^{-1})
A	0.024	0.061
B	0.064	0.048
C	0.121	0.063

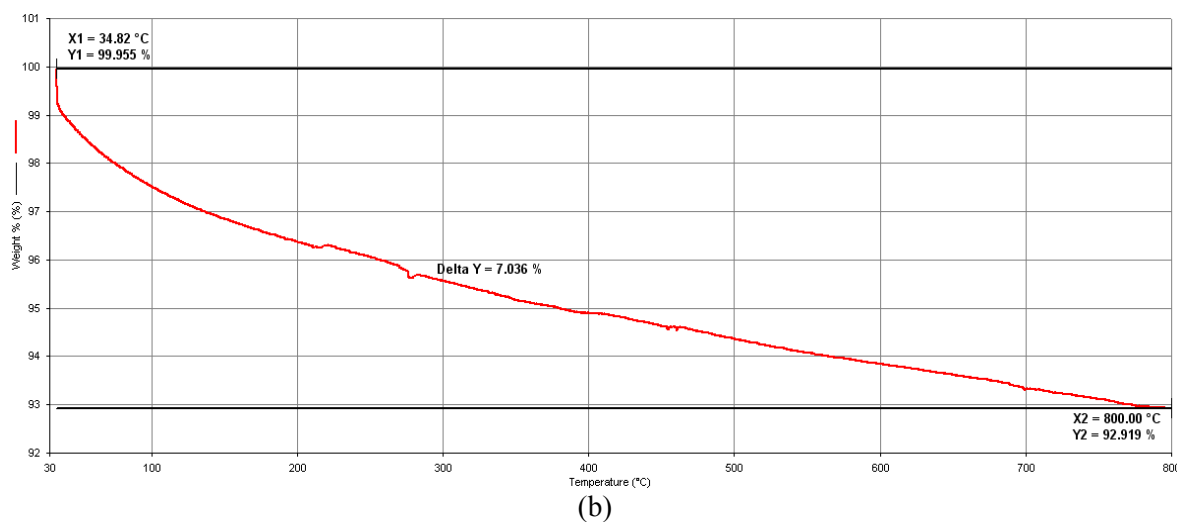
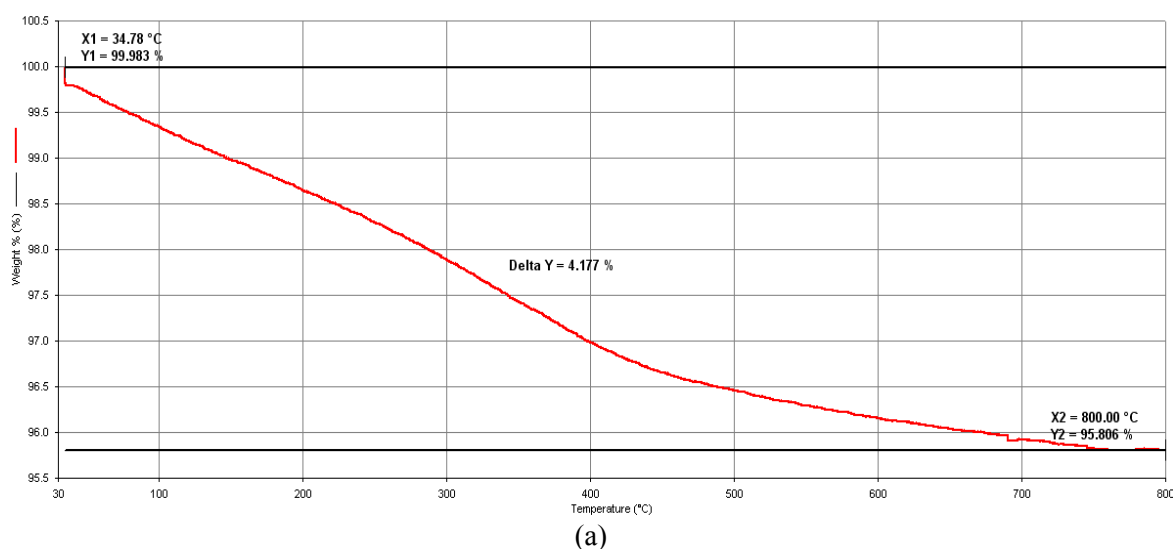
The TG/DTA profiles of the spent catalysts are depicted in Figure 5. The trend of profiles for all samples was the same indicating the

presence of a similar type of coke on catalysts. The amount of coke was in the order of: $B > C > A$.

As it is observed in Figure 5, in the temperature range of 30-800 °C, the weight losses of about 4.2 %, 7 % and 6.5 % were observed for the spent catalysts of samples A, B and C respectively. The lower the weight loss of a sample, the lower the amount of the deposited coke on the catalyst. Any weight loss in the temperature range of lower than 100 °C is related to the loss of humidity and any weight loss in the temperature range of 100-200 °C is due to the mobilization of light hydrocarbon depositions [16]. Moreover, it was reported [17] that any weight loss in the temperature range of 200-400°C is due to the deposition of soft hydrocarbons and any weight loss in the temperature range of 400-

600 °C is due to the deposition of hard and graphite-like hydrocarbons. As it is observed in Figure 5 and Table 4, most of the weight losses are observed in the temperature range of 200-400 °C that confirms the presence of soft cokes which can be omitted in the regeneration cycle.

Surprisingly, the catalyst stability does not correlate with the amount of coke. This implies that the coke deposition profiles have been different in different samples. Thus, compared to other samples, in sample B, being more affected by coke, the coke deposition should be more concentrated in the central parts of catalyst pellets compared to other samples.



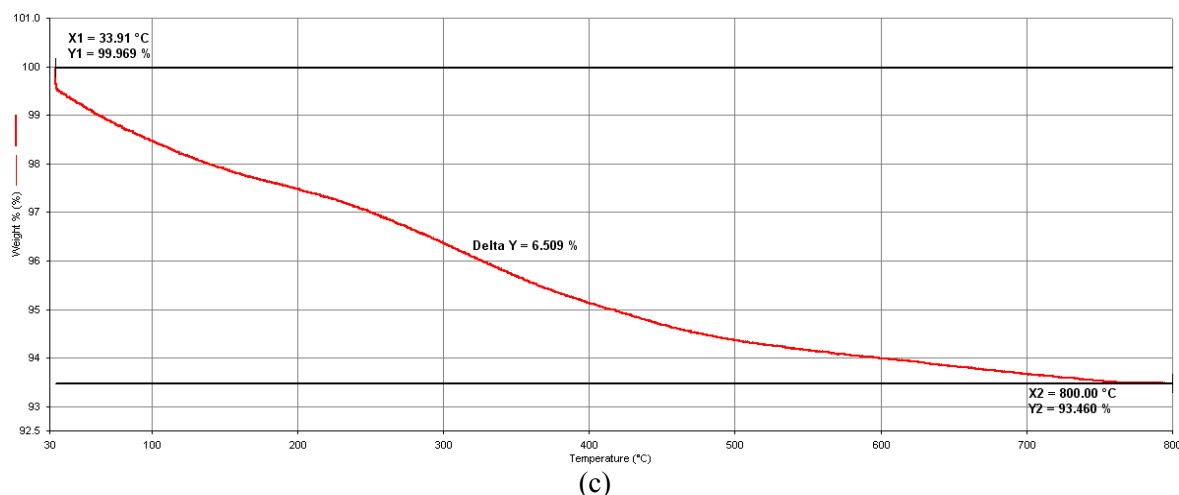


Figure 5. Coke deposition behavior (TG patterns) for the used catalysts after being on stream; (a) Sample A, (b) Sample B and (c) Sample C.

Table 4

Weight loss in different temperature ranges for used samples.

Sample	Weight loss (%)		
	100-200 °C	200-400 °C	400-600 °C
A	0.7	1.65	0.6
B	1.2	1.50	1.0
C	1.0	2.35	1.1

5. Conclusions

The rate of the addition of the PdCl_4^{2-} precursor to the impregnation solution during the preparation of the $\text{Pd-Ag/Al}_2\text{O}_3$ catalyst affects the distribution, penetration depth and dispersion of the Pd active metal and thus the performance of the catalyst in the selective hydrogenation of acetylene. The desirable egg-shell distribution prevails although it broadens by slowing down the rate of addition. This is due to the much higher rate of adsorption of Pd from the impregnation solution by the support compared to its diffusion rate within the support pores. However, for a given Pd loading, a too thin egg-shell results in the close proximity of Pd atoms favoring their agglomeration to larger ensembles which reduces the active metal surface area and promotes undesirable deep hydrogenation consecutive reactions.

Consequently, an optimum Pd penetration depth ($\sim 11 \mu\text{m}$ in this work) should be achieved by the controlled addition of precursors to maximize the ethylene selectivity.

References

- [1] Takht Ravanchi, M., Sahebdehfar, S. and Komeili, S., "Acetylene selective hydrogenation: A technical review on catalytic aspects", *Rev. Chem. Eng.*, **34**, 215 (2018).
- [2] Komhom, S., Mekasuwandumrong, O., Praserttham, P. and Panpranot, J., "Improvement of $\text{Pd/Al}_2\text{O}_3$ catalyst performance in selective acetylene hydrogenation using mixed phases Al_2O_3 support", *Catal. Commun.*, **10**, 86 (2008).
- [3] Kim W. J. and Moon S. H., "Modified Pd catalysts for the selective hydrogenation

- of acetylene”, *Catal. Today*, **185**, 2 (2012).
- [4] Panpranot, J., Aungkapipattanachai, S., Sangvanich, T., Boonyaporn, P. and Praserthdam, P., “Effect of N₂O pretreatment on fresh and regenerated Pd-Ag/ α -Al₂O₃ catalysts during selective hydrogenation of acetylene”, *React. Kinet. Catal. Lett.*, **91**, 195 (2007).
- [5] Gao, J., Zhu, Q., Wen, L. and Chen, J., “TiO₂-modified nano-egg-shell Pd catalyst for selective hydrogenation of acetylene”, *Particuology*, **8**, 251 (2010).
- [6] Pachulski, A., Schödel, R. and Claus, P., “Performance and regeneration studies of Pd-Ag/Al₂O₃ catalysts for the selective hydrogenation of acetylene”, *Appl. Catal. A: Gen.*, **400**, 14 (2011).
- [7] Tyurina, L. A., Nikolaev, S. A., Gurevich, S. A., Kozhevnikov, V. M., Smirnov, V. V. and Zhanavskiy, K. L., “Selective hydrogenation of acetylene on nanosized catalysts”, *Catal. Ind.*, **1**, 179 (2009).
- [8] Balint, I., Miyazaki, A. and Aika, K., “Alumina dissolution during impregnation with PdCl₄²⁻ in the acid pH range”, *Chem. Mater.*, **13**, 932 (2001).
- [9] Takht Ravanchi, M., Abedini, A., Sahebdehfar, S., Mehrazma, Sh. and Seyyed Shahabi, S., “Mathematical modeling of platinum and chlorine distributions within Pt-Sn/Al₂O₃ catalyst prepared by impregnation”, *Sci. Iran. C*, **22**, 981 (2015).
- [10] Anderson, J. R. and Pratt, K. C., Introduction to characterization and testing of catalyst, 2nd ed., Academic Press, Australia, (1985).
- [11] Takht Ravanchi, M., Sahebdehfar, S., Rahimi Fard, M., Fadaeeraeyeni, S. and Bigdeli P., “An experimental and modeling investigation on catalyst deactivation for Pd-Ag/ α -Al₂O₃ for acetylene selective hydrogenation”, *Chem. Eng. Tech.*, **39**, 301 (2016).
- [12] Bos, A. N. R. and Westerterp, K. R., “Mechanism and kinetics of the selective hydrogenation of ethyne and ethane”, *Chem. Eng. Proc. Proc. Int.*, **32**, 1 (1993).
- [13] Ludwig, W., Savara, A., Madix, R. J., Schauermaier, S. and Freund, H. -J., “Subsurface hydrogen diffusion into Pd nanoparticles: Role of low-coordinated surface sites and facilitation by carbon”, *J. Phys. Chem. C*, **116**, 3539 (2012).
- [14] Borodziński, A. and Bond, G. C., “Selective hydrogenation of ethyne in ethene-rich streams on palladium catalysts, Part 2: Steady-state kinetics and effects of palladium particle size, carbon monoxide, and promoters”, *Catal. Rev. Sci. Eng.*, **50**, 379 (2008).
- [15] Ahn, I. Y., Lee, J. H., Kim, S. K. and Moon, S. H., “Three-stage deactivation of Pd/SiO₂ and Pd-Ag/SiO₂ catalysts during the selective hydrogenation of acetylene”, *Appl. Catal. A: Gen.*, **360**, 38 (2009).
- [16] Sangkham, T., Mekasuwandumrong, O., Praserthdam, P. and Panpranot, J., “Effect of Fe-modified α -Al₂O₃ on the properties of Pd/ α -Al₂O₃ catalysts in selective acetylene hydrogenation”, *React. Kinet. Catal. Lett.*, **97**, 115 (2009).
- [17] Woo, K. J. and Sang, M. H., “Modified Pd catalysts for the selective hydrogenation of acetylene”, *Catal. Today*, **185**, 2 (2012).